2022-8

A Physical Layer Security (PLS) approach through Address Fed Mapping Crest Factor Reduction applicable for 5G/6G signals

Somayeh Mohammady
Technological University Dublin, somayeh.mohammady@tudublin.ie

David Malone Prof.
National University of Ireland, Maynooth, david.malone@mu.ie

Recommended Citation

S. Mohammady and D. Malone, "A Physical Layer Security (PLS) approach through Address Fed Mapping Crest Factor Reduction applicable for 5G/6G signals," 2022 9th International Conference on Future Internet of Things and Cloud (FiCloud), 2022, pp. 282-288, doi: 10.1109/FiCloud57274.2022.00047.

Funder: Science Foundation Ireland

A Physical Layer Security (PLS) approach through Address Fed Mapping Crest Factor Reduction applicable for 5G/6G signals

Somayeh Mohammady*, David Malone†
* School of Electrical & Electronic Engineering, Technological University Dublin (TU Dublin), Ireland
† Hamilton Institute/Department of Maths and Stats, Maynooth University, Kildare, Ireland
E-mail: somayeh.mohammady@tudublin.ie, david.malone@mu.ie

***Abstract*—The privacy and security of 5G/6G infrastructures are receiving great attention together with power consumption and efficiency. Here, Physical Layer Security (PLS) is considered and a technique named Address Fed Mapping (AFM) is proposed which not only enhances the physical layer security, but also reduces the effect of high Peak to Average Power Ratio (PAPR), which results in efficiency improvement in OFDM based signals used in beyond 5G and 6G [1]. The AFM is designed based on the idea of randomly generated signals, modifying the original signal to reduce PAPR. Instead of a typical randomization algorithm, a unique key is generated based on Channel response that is known only transmitter-receiver pairs. This key is used to pick a signal and send it. It is shown that the proposed AFM technique reduces PAPR, which improves the energy efficiency of the system.**

***Index Terms*—Channel response, CFR, PAPR, Physical layer Security, PLS, 5G and 6G**

I. Introduction

A. Security and Channel Response

Beyond 5G systems are expected to carry a variety of important traffic, including network control traffic, so it is important to provide secured transmission in order to prevent attacks on user, control and management traffic [2]. As discussed by the technical report released by the UK Department for Digital, Culture, Media and Sport of the United Kingdom government [3], 5G architectures should consider the principles of Cross-layer security, End-to-end security, Cross-domain security and Secure-by-design, as well as layer functions such as cell search [4]. Moreover, any modification added to the Physical layer or MAC layer, such as rotating the OFDM symbols or machine learning approaches on MAC layer, should be feasible and practical in terms of complexity and cost [5]. This is the main motivation behind designing AFM algorithm as it targets two points: improving the power efficiency by reducing the peak to average ratio and enhancing the security by making use of a parameter that is naturally random and available to use. This parameter, Channel Response [6], [7], looks at natural characteristics, such as time variability, and short time reciprocity [3] associated with the wireless communication medium. Designers often try to compensate for these characteristics by cancelling them, in order to enhance the connection. This means that the effect of he channel is treated as a distortion or noise. However, from security point of view, these natural characteristic can be used as temporary keys to protect the connection, which continuously changes naturally with no way of predicting by other unauthorized parties. Many works using Channel State Information (CSI) as a key to encrypt the signal [8], [9]. It has the benefit of being random by nature, and being known by the transmitter and receiver that have carried out the process of pairing. A typical example of a connection is presented in Fig. 1. Emily and Jack have to initialize a connection by sending training sequence, and then the channel characteristics will be known.

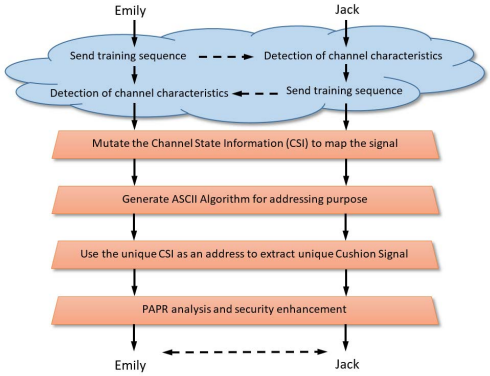

Fig. 1. Coherent Channel Response detection diagram

In this paper, it is assumed that the connection between Emily and Jack has been initialized, meaning that the channel response is known by both and the aim is that the connection stays secure. Our test set up is illustrated in Fig. 2, and Fig. 3, where a Chirp pulse is transmitted within 1 $meter$ distance, and the channel response is measured with an FPGA evaluation boards as shown (details in [10], [11]).

B. Efficiency and Peak to Average Power Ratio (PAPR)

An important aspect of any OFDM based technology, e.g. 5G and 6G mobile systems, is power efficient transmitters. In

Thanks Prasidh Ramabadram for help during the measurements and hardware tests. This publication has emanated from research conducted while working under the supervision of Prof. Ronan Farrell and Dr. John Dooley at Maynooth University and supported by the Science Foundation Ireland Research Centre for Future Networks and Communications (CONNECT).

978-1-6654-9350-5/22/$31.00 ©2022 IEEE
DOI 10.1109/FiCloud57274.2022.00047

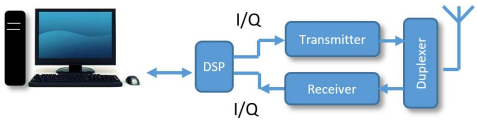

Fig. 2. Test Set up for capturing Channel Response

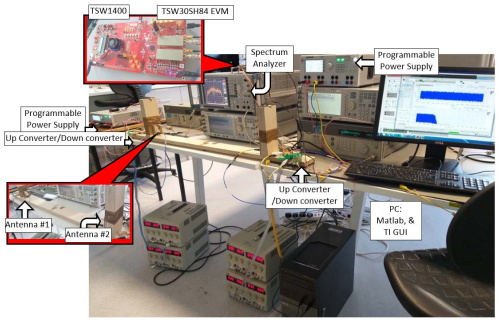

Fig. 3. Lab test Set up picture for capturing Channel Response

order to support the range of applications intended for beyond 5G, such as high speed enhanced Mobile Broadband(eMBB) [12], massive Machine-Type Communications (mMTC) [13], Augmented Reality and Virtual Reality AR/VR media, and Ultra-Reliable Low-Latency Communication (URLLC) [14], optimizing the transmitted power at the amplification stage is a major challenge [15]. However designing Radio Frequency (RF) components capable of that capacity is challenging when power consumption and efficiency is considered. The RF Power Amplifier (PA) is normally the component that dominates overall system power consumption [16]. Power efficiency of the PA can be degraded by properties of the amplified signal including Peak to Average power Ratio (PAPR) [17]–[19], which increases with bandwidth and length of Inverse Fast Fourier Transform (IFFT) [20]. A waveform that exhibits high PAPR degrades PA efficiency and linearity [14], [21]. As a logarithmic parameter, PAPR is a ratio between maximum power of the signal and average power,

$$PAPR_{dB} = 10\log_{10}\left(\frac{\text{Maximum Power}}{\text{Average Power}}\right). \quad (1)$$

As the occurrence of high PAPR depends on the signal, the probability of PAPR is considered [22]. This probability is measured with Complementary Cumulative Distribute Function (CCDF).

$$CCDF = \mathbb{P}\left(PAPR_{dB} > PAPR_{Threshold}\right). \quad (2)$$

A typical LTE (4G) signal with Bandwidth of 20MHz and IFFT length of 2048, has about 12.6dB PAPR at CCDF of 10^{-4}, meaning that the probability of occurrence of 12.6dB PAPR is about 0.1% for this signal (c.f. Fig. 4).

Fig. 4 presents CCDF plot for PAPR of OFDM signals with various IFFT lengths. Observe that as IFFT length increases, PAPR increases [23]. Tab. I shows this in another way, showing that PAPR increases with increase in bandwidth/IFFT

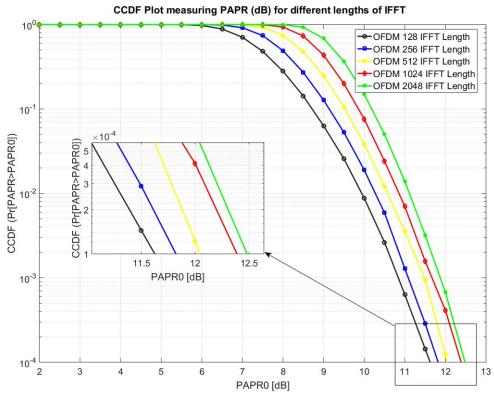

Fig. 4. CCDF, Probability of PAPR for different IFFT Length Signals

Bandwidth	IFFT Length	PAPR	Efficiency η
1.4 MHz	128	11.636 dB	13.10%
3 MHz	256	11.84 dB	12.79%
5 MHz	512	12.061 dB	12.47%
10 MHz	1024	12.401 dB	11.99%
15 MHz	2048	12.503 dB	11.85%
20 MHz	2048	12.61 dB	11.71%

TABLE I
BANDWIDTH, IFFT LENGTH OF LTE SIGNAL, AND CORRESPONDING PAPR (DB)

length. 5G signals are expected to have bandwidth of between 50–400 MHz, so it is clear that the PAPR becomes more important than ever. This can be also observed from Fig. 5, which presents plots showing measured PAPR and a a linear model. By assuming $BW = 50MHz$, the the linear model will be 15.3dB. Equally, for an IFFT length of 8192, the PAPR would be 15.7dB. The direct effect of high PAPR is on PA efficiency, but here this concern is addressed together with the security of transmission.

The energy efficiency η is used in power analysis when designing transmission systems. A significant portion of power is wasted as heat in PAs and bulky heat sinks are often used to manage the heat [24], [25]. High efficiency systems should maximise the power of the output signal relative to input signal [26], which can be captured by optimising η

$$\eta = \frac{P_{Output}}{P_{Input}}, \quad (3)$$

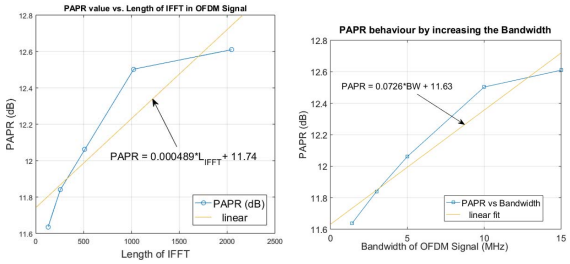

Fig. 5. PAPR value vs. Length of IFFT/Bandwidth in OFDM Signal

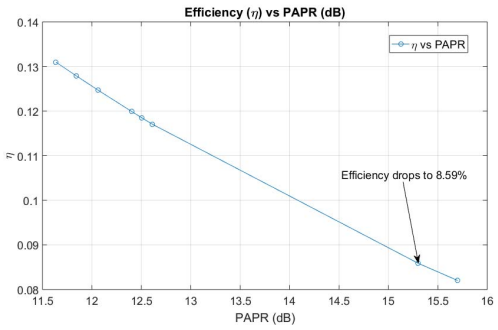

Fig. 6. Efficiency (η) vs. PAPR (dB)

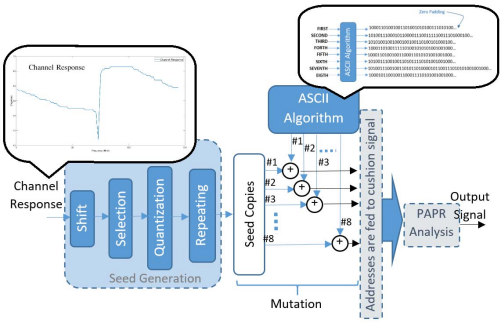

Fig. 7. The AFM block diagram

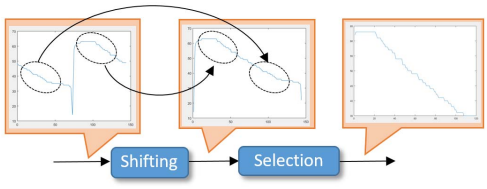

Fig. 8. Shifting, and Selection process in Seed Generation

where P_{Output} is the power for output signal, and P_{Input}, is the power for input signal. Note that η typically behaves exponentially with values of PAPR in dB,

$$\eta(PAPR) = \eta_0 10^{\frac{-PAPR}{20}}. \quad (4)$$

If $PAPR = 0$, $\eta = \eta_0$ which is the initial energy efficiency of PA. Here we use the assumption that η_0 is 50% [26], [27]. With this, energy efficiency can be calculated (see Tab. I and Fig. 6). By assuming $PAPR = 15.3$dB, we see η drops to 8.59%, which is undesirable.

There are works targeting both PAPR reduction and security. For example, in [9], the Selected Mapping (SLM) [28] technique is used to encrypt the signal. However, when generating ransom phases for the SLM technique [29], there is a chance that the original signal, which has no phase rotation, has minimum PAPR, and is selected to be sent [30]. From security point of view, the signal can be revealed. Moreover, the receiver has to be informed about the SLM selection for every single transmission. This information, known as side information [31], usually consist of few bits, however, they are crucial key to reveal the signal, and channel security for these bits are necessary.

In this paper, a new algorithm is developed in order to enhance the security through a system that reduces the PAPR of a signal prior passing through PA. The new algorithm, Address Fed Mapping (AFM), is shown to be a feasible solution to target both security and PAPR of transmitter and it is capable of processing 4G and 5G signals.

II. Address Fed Mapping (AFM)

As mentioned before, the initial idea is to use the channel response as a key. The benefit, as mentioned earlier, is that the key is known by transmitter and receiver. The nature of the channel response makes it a suitable key. The first block in main block diagram presented in Fig. 7, indicated by Seed Generation shows four steps of Shifting, Selection, Quantization, and Repeating.

A. Seed Generation

As seen in Fig. 7, the channel response has a drop in the middle, which is due to DC offset. When this data is shifted, the channel response usage is more efficient, meaning that the deep drop on the left of Fig. 7 joins more smoothly to the right. The shifted process, which rearranges zero frequency components in correct order, can be used to generate keys.

The next step in our scheme is selection, which means that the usable area of the the plot is selected, as shown in Fig. 8. The selection process is used to avoid flat responses, as when quantized a flat response will produce similar values, which is not desirable for randomization. The quantization process can be easily implemented in simulation by normalizing the values, and slicing the values, and so producing the seed. The process of repeating the seed is performed in order to ensure that the length of the input signal matches the length of the seed that is being produced. The effect of repeating can be also seen in Fig. 9. This seed is then used for mutation as seen in middle section of the block diagram Fig. 7.

B. Mutation Process

This part of the algorithm is inspired by the SLM approach, [28], and also indirectly from Genetic Algorithms. In the SLM technique, there are copies of the original sequence and

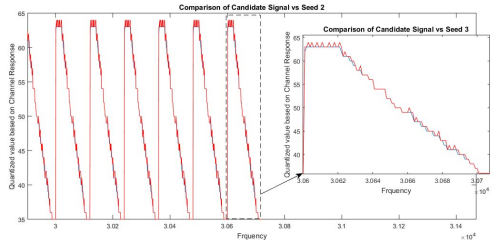

Fig. 9. Candidate Signal vs Seed

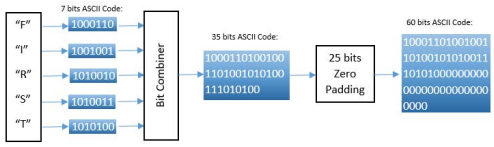

Fig. 10. ASCII Converter Algorithm

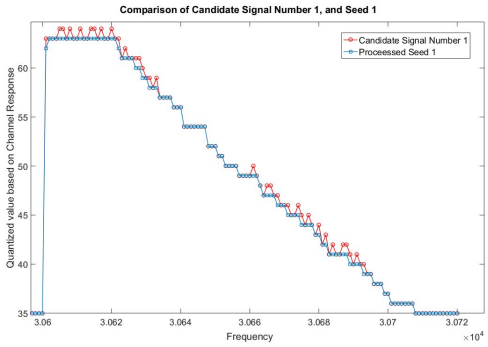

Fig. 11. Comparison of Candidate Signal 1 vs Seed 1

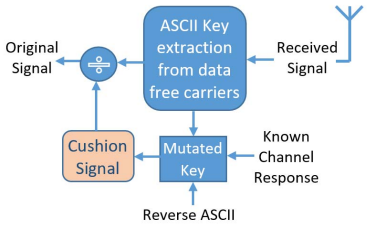

Fig. 12. AFM receiver block diagram

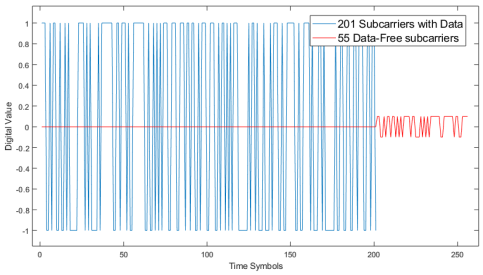

Fig. 13. OFDM signal indicating data free sub carriers

multiplications modify them in order to find the best sequence in terms of PAPR value. Here the seed that was generated by the previous section is fed to this mutation process inspired by Genetic algorithm. The seed is copied M times (in this paper, $M = 8$), and mutated. This mutation is performed by American Standard Code for Information Interchange (ASCII) [32] algorithm, as instead of the usual multiplication, here there are 8 complex additions, and instead of phase rotation, ASCII algorithm is used in order to form an encoding process. The initial assumption behind the design of the proposed AFM technique, is that the seed is known by transmitter, and receiver, therefore, in order to have multiple versions of the seed which means multiple addresses for picking up values from the designed cushion signal, as shown in Fig. 10, ASCII algorithm is used to generate unique identification for each address. This encodes the message in a unique manner that only receiver would be able to decode.

The main idea behind using ASCII algorithm here is to give each sequence an identity that can be easily extracted by the receiver. It should be noted that this part does not require significant security, as the addresses sequence is secured, and the seed that generates each address is also secured, so the main purpose of the design is to have clear identification. This process will enhance the security of the signal, and informs the receiver about the selection on transmitter side by this identity. The process of ASCII is shown in Fig. 7.

The idea of using ASCII algorithm is also inspired by some works that suggest the use of a pattern in SLM, in order to avoid side information [18], [33]. Here the idea helps the AFM algorithm to be enhanced and also does not need transmission of extra bits with highly secure channel. The effect of mutation can be seen by red color variation around the blue plots in Fig. 11 and Fig. 9. It should be noted that the sequence generated for identifying the selected signal is a result of the addition of ASCII bits and the seed generated from the channel response. This pattern should be stored at the receiver, and when receiving the encrypted signal, having both the pattern and channel response, the receiver is able to extract the original signal. This is only possible for the paired receiver. The process of extracting original signal by using the known channel response, and the key to reversing the ASCII algorithm is shown in Fig. 12. Note that the key for ASCII does not require significant security, since it only addresses the sequence generated based on Cushion signal, and the seed originated from channel response.

However, ensuring that correct address is sent to the receiver it crucial. Here it is recommended to send the address indicating the selection only for PAPR section, to the receiver using data-free sub-carriers in OFDM signal frame. An example plot is shown in Fig. 13, which shows that according to IEEE standard [34], from 256 sub-carriers in OFDM frame, 201 sub-carriers carry data, and 55 of them are known to be data-free sub-carriers, and they are designed to ensure space between channels. At the receiver, this section will be discarded after receiving the signal [30]. The idea is to make use of this space inspired by some of previous works [18], [33], as not all the space is required for transmitting the information for PAPR selection, but the benefit is that this band is secured together with the same data carrying sub-carriers, so there is no need for extra security. Where the data-free sub-carriers are discarded at the receiver, they are in fact recycled and the information for PAPR and the division for reverse process as shown in Fig. 12 is operated, and the signal can be securely extracted.

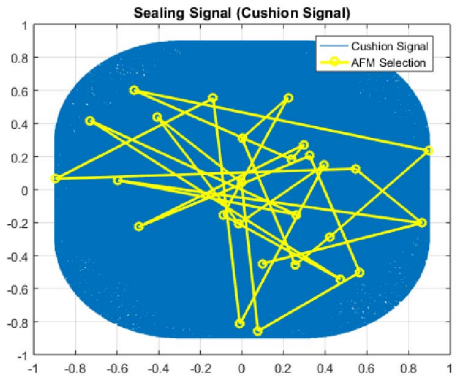

Fig. 14. Cushion Signal, and AFM selection path

C. Cushion Signal Generation

The main idea behind the Cushion shape signal is to seal the modulation scheme, as circle, square, or rectangle might categorize the probability of using QAM, QPSK, or OQPSK, and BPSK schemes. However, in this paper the cushion signal is purely used to generate completely random phase rotations with fed address that are only recognizable with receiver, resulting in enhancement of the security, and moreover reduction in PAPR. It should be noted the proposed technique is applied to the signal after modulation, not instead of modulation, therefore, the constellations are assumed to be changed and it is important to reverse the process as shown in Fig. 12, right after receiving the signal at the receiver side and before demodulation process, in order to have correct constellation detection. When comparing the path indicated by yellow lines in Fig. 14, and the path in both cases of QPSK, and OPSK in Fig. 15, it can be observed that the path that the randomization takes is lot more predictable in SLM-based approaches. In contrast, the path that randomization presented in cushion signal, as shown in Fig. 15, indicates that the only way of extracting the correct path is by having the key that is generated by the common channel response. The idea of sealing the modulation scheme by using the cushion signal (detailed below) can be explored further in future works. It should be noted that it is assumed that the cushion signal is known by the paired transmitter, and receiver.

As shown in Fig. 12, once the address is generated by the seed it is used to pick up a value from the cushion. The cushion signal is generated using

$$C = a + ib, \tag{5}$$

where a and b are the real and imaginary parts of signal and can be determined using

$$\begin{aligned} a &= r\cos\theta_a + \beta_a \\ b &= r\cos\theta_b + \beta_b \end{aligned} \tag{6}$$

where r is the radius for our cushion signal, and here $r = 0.3$, the angle θ varies from 0 to 2π, with step size of π/α. α

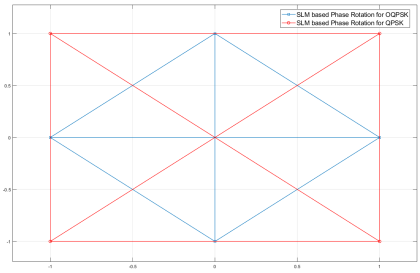

Fig. 15. Phase rotations based on SLM based techniques

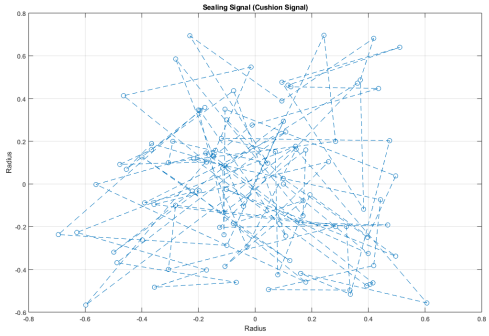

Fig. 16. Example of Cushion Signal with $Num = 100$, and $r = 0.2$

indicates the quantity of varied phases, calculated by $(Num-1)/2$, and Num should be same length as the input signal. In this paper the LTE toolbox is used to generate the input signal, $Num = 30720$. An example when $r = 0.2$, and $Num = 100$ is presented in Fig. 16.

From the Cartesian point of view, the cordinates, (x, y), of each point on Fig. 17 are selected by further randomization as x and y are generated randomly as:

$$\begin{aligned} x &= (\text{random values between -1 and 1}) \times s_h \\ y &= (\text{random values between -1 and 1}) \times s_h \end{aligned} \tag{7}$$

where s_h is the size of the center point, shown by a hole in Fig. 17. It should be noted that the range of (-1) and $(+1)$ are selected on purpose in order to avoid additional peaks in signal, and covering all possible points generated by any mentioned type of modulation scheme. It should be also noted that, for this work in most of the cases, and in most of results presented in this paper, $s_h = 0.3$, which means that there is no hole, and random values are allowed to cross zero as shown in Fig. 16 and Fig. 14. However in some cases, for example in out-phasing power amplifiers (PAs), when the bandwidth is expanded and distortion around the main spectrum is experienced which is due to the signal being close to zero, s_h can be increased which means that zero crossing can be avoided which is shown in Fig. 17. This will result in distortion reduction caused by out-phased signals [35], however here this case is not the concerned.

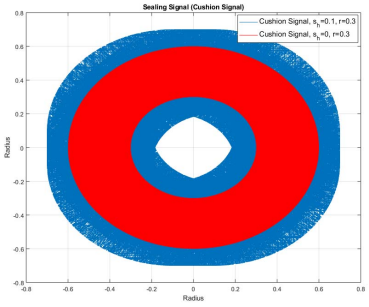

Fig. 17. Cushion Signal when s_h is varied

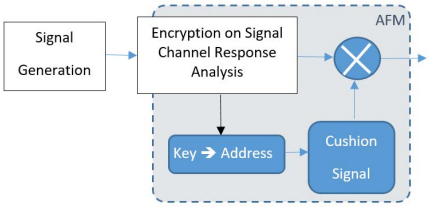

Fig. 18. AFM technique block diagram

III. Performance Analysis

We tested the AFM technique with more than 10^5 OFDM-based signals. CCDF results are presented in Fig. 19. Observe that as seen in Fig. 4, the original OFDM signal presents about $12.5dB$ PAPR at CCDF of 0.0001. By applying the proposed AFM technique, this value is reduced to $10.5dB$, $10.3dB$, $10.3dB$, $9.8dB$, and $5.7dB$, at a comparable point of $CCDF = 0.0001$. From eq. 4, the energy efficiency is consequently improved from 12.79% to 14.93%, when the IFFT length is 256, and only one additional phase from AFM technique is added. Tab. II presents more results achieved based on AFM, and calculation of efficiency based on PAPR.

To obtain the results in Fig. 4, the efficiency improvement is obtained by subtracting the achieved efficiency from the efficiency obtained from Eq. 4 using PAPR values without the AFM technique applied. Note that there are two selection when it comes to choosing the sequence with minimum PAPR, and the information indicating the selected sequence in this case would be $first$, or $second$, and in binary format it would be 01100110, for f, 01101001 for i, 01110010 for r, and so on. Another way of employing this idea would be to do it in numeric format, as $1st$ represented by 00000001, and $2nd$ with 00000010. However, note that the chance that in numeric format, any mistake in one bit only leads to failure in extracting the information at the receiver, the binary using letters is recommended. Moreover, a common understanding should be established at the beginning of connection between the transmitter, and the receiver, in order to agree to use capital letters, or small letters. For example 01100001 represents a, and 01000001 represents A, therefore, any confusion must be avoided.

IFFT Length	$PAPR_{AFM}$ at 10^{-4} CCDF	Achieved Efficiency Efficiency η Improvement
256	11.84 dB	12.79%
512	12.061 dB	12.47%
1024	12.401 dB	11.99%
2048	12.503 dB	11.85%

TABLE II
Energy Efficiency Improvement by Applying AFM technique

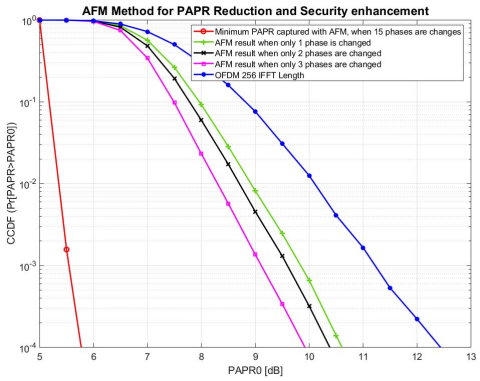

Fig. 19. CCDF plot for PAPR reduction effect of AFM technique

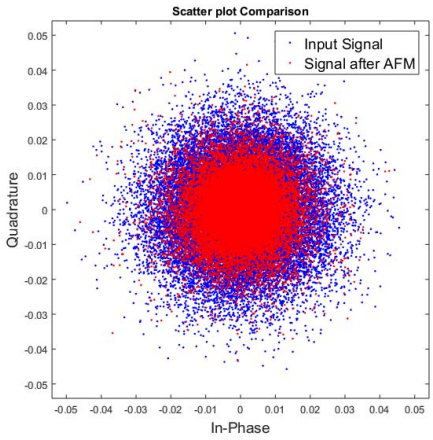

Fig. 20. Comparison of scatter-plots before and after AFM technique

As channel frequency response varies at each pairing, it is possible to use it as a factor to secure transmission. Here the source of the technique relies on this channel response, then as explained earlier, it is processed and a unique sequence is generated. The signal's scatter-plot with and without the AFM technique is compared in Fig. 20.

As seen in Fig. 20, the scatter-plot of the original signal indicated by blue color, varies from the processed signal indicated by red color. This indicates that only the paired receiver that has access to the exact same channel response, and exact same ASCII pattern, and exact same cushion signal can extract the signal.

IV. Conclusion

This paper introduces a technique for enhancing security at the physical layer for beyond 5G and 6G signals, and simultaneously reduces the PAPR of the signal and leads to improved power efficiency. The proposed methods are explained and simulation results show $3dB$ reduction in PAPR at CCDF of 10^{-4}, resulting directly in an improvement in energy efficiency, and enhancement in the security from physical layer point of view. The idea blends the natural randomization of channel response with phase rotations based on this randomization, which also reduces PAPR. This technique has potential to be applied to completely seal the modulation scheme which can be explored in future work. Furthermore, It would be interesting to study the practicality of guessing attacks on either the channel, seed or key in the future.

References

[1] X. Li, J. Huang, Y. Lyu, R. Ni, J. Luo, and J. Zhang, "Two types of mixed orthogonal frequency division multiplexing (X-OFDM) waveforms for optical wireless communication," *IEEE Transactions on Wireless Communications*, vol. 21, no. 2, pp. 1092–1102, 2022.

[2] Z. Wei, F. Liu, C. Masouros, N. Su, and A. P. Petropulu, "Toward multifunctional 6G wireless networks: Integrating sensing, communication, and security," *IEEE Communications Magazine*, vol. 60, no. 4, pp. 65–71, 2022.

[3] *Technical Report on 5G Network Architecture and Security A collaborative paper DCMS Phase 1 5G Testbeds & Trials Programme*, Department for Digital, Culture, Media and Sport of the United Kingdom government, 2018, https://uk5g.org, and https://www.gov.uk.

[4] G. Gür, "Expansive networks: Exploiting spectrum sharing for capacity boost and 6G vision," *Journal of Communications and Networks*, vol. 22, no. 6, pp. 444–454, 2020.

[5] A. K. Yerrapragada, T. Eisman, and B. Kelley, "Physical layer security for beyond 5G: Ultra secure low latency communications," *IEEE Open Journal of the Communications Society*, vol. 2, pp. 2232–2242, 2021.

[6] W. Chang and J. R. Cruz, "Optimal channel detection for nonbinary coded partial response channels," *IEEE Transactions on Communications*, vol. 57, no. 7, pp. 1892–1895, 2009.

[7] M. Sun, G. Goussetis, K. Xu, Y. Ding, S. Mclaughlin, A. Segneri, and M. J. C. Sánchez, "Joint digital analogue DVB-S2(X) link optimization in non-linear channel," *IEEE Access*, vol. 10, pp. 40 794–40 805, 2022.

[8] K. Ren, H. Su, and Q. Wang, "Secret key generation exploiting channel characteristics in wireless communications," *IEEE Wireless Communications*, vol. 18, no. 4, pp. 6–12, August 2011.

[9] Y. Xiao, Z. Wang, J. Cao, R. Deng, Y. Liu, J. He, and L. Chen, "Time-frequency domain encryption with SLM scheme for physical-layer security in an OFDM-PON system," *IEEE/OSA Journal of Optical Communications and Networking*, vol. 10, no. 1, pp. 46–51, Jan 2018.

[10] P. Ramabadran, D. Malone, S. Madhuwantha, P. Afanasyev, R. Farrell, J. Dooley, and B. O'Brien, "A novel physical layer encryption scheme to counter eavesdroppers in wireless communications," in *2018 25th IEEE International Conference on Electronics, Circuits and Systems (ICECS)*, Dec 2018, pp. 69–72.

[11] P. Ramabadran, S. Madhuwantha, P. Afanasyev, R. Farrell, L. Marco, S. Pires, and J. Dooley, "Digitally assisted wideband compensation of parallel RF signal paths in a transmitter," in *2018 91st ARFTG Microwave Measurement Conference (ARFTG)*, June 2018, pp. 1–4.

[12] G. Liu, X. Hou, J. Jin, F. Wang, Q. Wang, Y. Hao, Y. Huang, X. Wang, X. Xiao, and A. Deng, "3-D-MIMO with massive antennas paves the way to 5G enhanced mobile broadband: From system design to field trials," *IEEE Journal on Selected Areas in Communications*, vol. 35, no. 6, pp. 1222–1233, June 2017.

[13] F. Yang and X. Wang, "A novel waveform for massive machine-type communications in 5G," in *2017 IEEE Wireless Communications and Networking Conference (WCNC)*, March 2017, pp. 1–5.

[14] H. Malik, M. M. Alam, Y. Le Moullec, and Q. Ni, "Interference-aware radio resource allocation for 5G ultra-reliable low-latency communication," in *2018 IEEE Globecom Workshops (GC Wkshps)*, Dec 2018, pp. 1–6.

[15] T. E. Abrudan, S. Kucera, and H. Claussen, "Unitary checkerboard precoded OFDM for low-papr optical wireless communications," *Journal of Optical Communications and Networking*, vol. 14, no. 4, pp. 153–164, 2022.

[16] H. Wang, P. M. Asbeck, and C. Fager, "Millimeter-wave power amplifier integrated circuits for high dynamic range signals," *IEEE Journal of Microwaves*, vol. 1, no. 1, pp. 299–316, 2021.

[17] S. Mohammady, R. Farrell, D. Malone, and J. Dooley, "Peak shrinking and interpolating technique for reducing peak to average power ratio," in *2019 Wireless Days (WD)*, April 2019, pp. 1–6.

[18] S. Razavi, N. Sulaiman, R. M. Sidek, S. Mohammady, and P. Varahram, "Analysis on the parameters of selected mapping without side information on papr performances," in *2014 IEEE 5th Control and System Graduate Research Colloquium*, Aug 2014, pp. 43–46.

[19] S. Narahashi and T. Nojima, "New phasing scheme of n-multiple carriers for reducing peak-to-average power ratio," *Electronics Letters*, vol. 30, no. 17, pp. 1382–1383, Aug 1994.

[20] R. Niwareeba, M. A. Cox, and L. Cheng, "PAPR reduction in optical OFDM using lexicographical permutations with low complexity," *IEEE Access*, vol. 10, pp. 1706–1713, 2022.

[21] D. Y. C. Lie, J. C. Mayeda, and J. Lopez, "Highly efficient 5G linear power amplifiers (PA) design challenges," in *2017 International Symposium on VLSI Design, Automation and Test (VLSI-DAT)*, April 2017, pp. 1–3.

[22] W. P. Huang J., Zhou S., "Nonbinary LDPC coding for multicarrier underwater acoustic communications," in *OCEANS'08 MTS/IEEE Kobe-Techno-Ocean'08- Voyage Toward the Future (OTO'08)*, Japan, 2008, https://www.tib.eu/en/.

[23] W. Tsai, C. Liou, Z. Peng, and S. Mao, "Wide-bandwidth and high-linearity envelope- tracking front-end module for LTE-A carrier aggregation applications," *IEEE Transactions on Microwave Theory and Techniques*, vol. 65, no. 11, pp. 4657–4668, Nov 2017.

[24] N. J. Kolias and R. C. Compton, "Thermal management for high-power active amplifier arrays," *IEEE Transactions on Microwave Theory and Techniques*, vol. 44, no. 6, pp. 963–966, June 1996.

[25] Xin Jiang, Li Liu, S. C. Ortiz, R. Bashirullah, and A. Mortazawi, "A ka-band power amplifier based on a low-profile slotted-waveguide power-combining/dividing circuit," *IEEE Transactions on Microwave Theory and Techniques*, vol. 51, no. 1, pp. 144–147, Jan 2003.

[26] S. R. Biyabani, R. Khan, M. M. Alam, A. A. Biyabani, and E. McCune, "Energy efficiency evaluation of linear transmitters for 5G NR wireless waveforms," *IEEE Transactions on Green Communications and Networking*, vol. 3, no. 2, pp. 446–454, June 2019.

[27] S. L. Miller and R. J. O'Dea, "Peak power and bandwidth efficient linear modulation," *IEEE Transactions on Communications*, vol. 46, no. 12, pp. 1639–1648, Dec 1998.

[28] R. W. Bauml, R. F. H. Fischer, and J. B. Huber, "Reducing the peak-to-average power ratio of multicarrier modulation by selected mapping," *Electronics Letters*, vol. 32, no. 22, pp. 2056–2057, Oct 1996.

[29] S. Mohammady, N. Sulaiman, P. Varahram, R. M. Sidek, and M. N. Hamidon, "Performance investigation between DSI-SLM and DSI-PTS schemes in ofdm signals," in *2012 International Symposium on Telecommunication Technologies*, Nov 2012, pp. 210–214.

[30] *Peak to Average Power Ratio Reduction based on optimum phase sequence in Orthogonal Frequency Division Multiplexing Systems*. [Online]. Available: http://psasir.upm.edu.my/id/eprint/38550/1/FK%202012%2020R.pdf

[31] S. Mohammady, R. M. Sidek, P. Varahram, M. N. Hamidon, and N. Sulaiman, "A new DSI-SLM method for PAPR reduction in OFDM systems," in *2011 IEEE International Conference on Consumer Electronics (ICCE)*, Jan 2011, pp. 369–370.

[32] C. E. Mackenzie, *Coded Character Sets, History and Development*. New York: IBM Corporation Addison, 1980.

[33] S. Razavi, N. Sulaiman, S. Mohammady, R. M. Sidek, and P. Varahram, "Efficiency analysis of papr reduction schemes," in *2012 International Symposium on Telecommunication Technologies*, Nov 2012, pp. 279–284.

[34] *IEEE 802.16e WiMAX OFDMA Signal Measurements and Troubleshootin*, IEEE standards, USA, 2011, agilent Application Note 1578.

[35] K. Finnerty, *Linear Operation of Switch-Mode Outphasing Power Amplifiers*, 2016.